EXPERIMENTAL AND NUMERICAL INVESTIGATION OF FIBER REINFORCED COMPOSITE FLOATING BARRIER

Lyka Yvonne O. Victoria*, Ella G. Vargas, Ana Carmela V. Malpaya Glecy C. Malibiran, Nicole M. Hernandez, Mary Glen L. Caugma
Bachelor of Science in Civil Engineering
College of Engineering
Occidental Mindoro State University
**victorialykayvonne@gmail.com*

ABSTRACT

The study suggested the implementation of a sustainable floating barrier made of densified recycled plastics strengthened with treated coconut coir fiber, combining coastal protection and waste management through an experimental-computational method. Design-Expert was used to optimize the mixture designs, with mechanical behavior and wave attenuation studied with Finite Element Analysis and ANSYS Fluent. Laboratory tests on ASTM-based testing and the modified Rule of Mixtures were used to validate the numerical results. The optimized design mixture exhibited mechanical strength, water absorption, and durability with the conventional HDPE materials of density 0.848 g/cm3, water absorption of 0.63, and compressive strength of 3.98 MPa. The results in wave attenuation demonstrated 14.80%-26.57% reduction with a mean absolute percentage error of 12.29, showing a good correspondence of the numerical and experimental results.

Keywords: *floating barrier, wave attenuation, densified plastic, coconut coir fiber, Finite Element Analysis, Computational Fluid Dynamics*

SDG: *SDG 9: Industry, Innovation, and Infrastructure; SDG 13: Climate Action*

INTRODUCTION

The increase in vulnerability of the coastal regions to storm waves and erosion created more pressing demands for more effective sustainable coastal protection systems. These are the floating barriers to absorb the energy of the waves and protect the coastal structures and ecosystems (Edmonds et al., 2020; Reis et al., 2025). Defensive measures currently in place in the coastal areas have not been able to withstand extreme events leading to the need of stronger and more flexible actions (Estacio et al., 2025; GMA News, 2020). This need is particularly relevant in the Philippines, where long coastlines and frequent typhoons increase the risk of coastal damage and flooding (NASA, 2024; Nature Communications, 2022).

Meanwhile, mass amounts of plastic waste have been dumped into marine systems each year (United Nations Environment Programme, 2022). The Philippines is one of the most active sources of marine plastic pollution (Jambeck et al., 2015), showing the possibility of recycling waste materials. Recycled plastics, expanded polystyrene (EPS), and coconut coir fiber have been found to enhance compressive and tensile strength (Anggraini et al., 2015; Guruswamy et al., 2024), while coir fiber shows benefits in availability and sustainability. Furthermore, the natural fiber composites have been regarded as a promising source of marine engineering due to positive strength-to-weight ratio and sustainability advantages (El Hawary et al., 2023).

While densified plastics have been explored as a recycled material due to its structural stability and physical properties, most have primarily focused on material characterization with limited attention given to practical applications with numerical validation for marine applications particularly in coastal systems. The proposed study aims to produce mixtures of LDPE, EPS, waste cooking oil, and treated coconut coir fiber and numerically assess their mechanical performance using Fusion 360. This study contributes to the development of a sustainable floating barrier system while promoting plastic waste utilization.

METHODS

Research Design

The study employed an experimental-computational research design in which the floating plastic composite was developed and tested to evaluate its mechanical behavior and wave attenuation performance.

Project Development Methodology

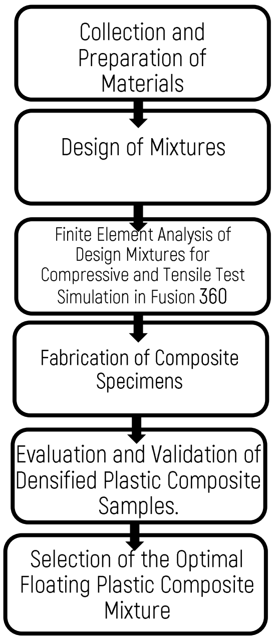

Figure 1. Flow chart of the project development methodology.

Collection and Preparation of Materials

a) Low-Density Polyethylene (LDPE) and Expanded Polystyrene (EPS)

Materials used were non-foil plastic wrappers, bubble wrap, and EPS. Gathered plastics were washed and dried to eliminate contaminants and moisture and shredded into particles.

b) Coconut Coir Fiber

The preparation of coconut coir fibers in this study followed the procedure described by Kondo et al. (2023). Fibers were washed, dried after 24 hours under air and cut to 30 mm length. Treated with 20 percent NaOH for three hours to eliminate lignin and impurities and rinsed and dried in the sun over 24 hours.

c) Used Cooking Oil

The oil was collected after the first use for cooking and stored temporarily in clean plastic containers.

Design of Mixtures

Response Surface Methodology (RSM) in Design-Expert software was used to formulate floating plastic composites. The mixture designs were constrained to total 100%, with densified LDPE and EPS ranging from 1–99% and treated coconut coir fiber limited to a maximum of 20%.

Finite Element Analysis of Design Mixtures for Compressive and Tensile Test Simulation in Fusion 360

A combined finite element analysis (FEA) and experimental approach was used to evaluate the mechanical behavior of coconut coir fiber–reinforced plastic composites. Autodesk Fusion 360 simulated ASTM compressive tensile tests using material properties estimated through the Rule of Mixtures (ROM). Mesh refinement was applied in critical regions.

Fabrication of Composite Specimens

Composite specimens were fabricated through a manual densification process using medium-sized stainless steel cooking ware. The volume of LDPE, EPS, and treated coconut coir fiber were measured with the amount of used cooking oil prepared in equal to the total mixture volume and used as the heating medium.

The oil was preheated to 100°C for 30 minutes prior to gradually adding shredded plastics. The densification process was maintained at 125–175°C using a food-grade thermometer for approximately 30 minutes until a uniform consistency was achieved, then poured into prepared molds. Treated coconut coir fiber was then added and manually mixed to ensure even distribution throughout the composite before allowing the specimens to set. Mold dimensions followed

Vol. 5, No. 1, June 2026 | pISSN:2980-4523 | eISSN: 3027-9054

ASTM standards: 50 mm × 50 mm × 50 mm for compressive strength specimens and 165 mm × 19 mm × 3.2 mm for tensile specimens with a 50 mm gauge length.

Evaluation and Validation of Densified Plastic Composite Samples

The densified plastic composites were evaluated through laboratory testing to validate their mechanical behavior. Tests were conducted in accordance with ASTM standards for density and specific gravity (ASTM D792), water absorption (ASTM D570), and compressive strength (ASTM C109). Tensile strength and other mechanical properties were estimated using the modified Rule of Mixtures (ROM) following Espinach et al. (2023). The mechanical properties of the densified plastic composite were estimated using the modified Rule of Mixtures (ROM). The matrix tensile strength was calculated using Equation 1.

$$\sigma_{Ct} = f_c \cdot \sigma_{Ft} V_F + \sigma_{Mt} V_M \quad - eq. 1$$

Where:

σ_{Ct} = predicted tensile strength of the composite
σ_{Ft} = tensile strength of the fiber
V_F = fiber volume fraction
$V_M = 1 - V_F$ = matrix volume fraction
f_c = fiber orientation efficiency factor

Each mixture was considered valid when the average experimental and empirical load fell within the nearest simulated load.

Selection of the Optimal Floating Plastic Composite Mixture

LDPE, EPS, and treated coconut coir fiber proportions were used as independent variables in Design-Expert RSM, while density, water absorption, compressive strength, and tensile strength as the response variables. Regression models were developed to predict material behavior, and prediction accuracy was evaluated using Relative Standard Error (RSE) which is given by Equation 2.

$$RSE\ (\%) = \frac{Actual\ Value - Predicted\ Value}{Predicted\ Value}\ x\ 100 \quad - eq. 2$$

Wave Attenuation Performance of Floating Plastic Composite Prototype

The testing was done in two complementary methods; a numerical simulation in ANSYS Fluent and experimental test in a flume tank in different conditions of waves. The most significant parameters taken in the research were incident wave height (Hi), transmitted wave height (Ht), wave transmission coefficient (Kt) and wave reduction (WR).

Numerical Simulation of Wave Attenuation

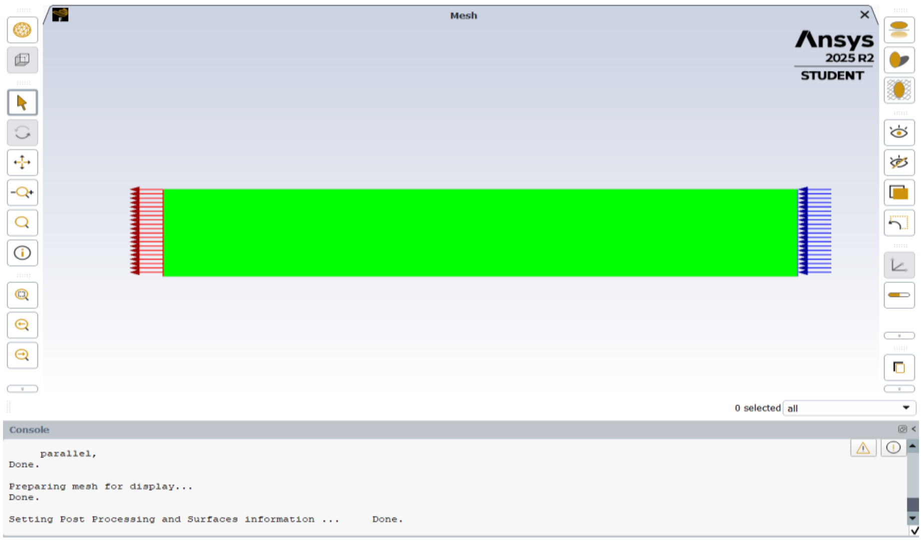

Figure 2. Flow direction from inlet to outlet from ANSYS.

Using Computational Fluid Dynamics (CFD) software, ANSYS Fluent, a transient two-phase flow model is used to compute the wave–structure interaction and to analyse the hydraulic performance of the floating densified plastic composite, assuming gravity and rigid body. The simulation domain was a wave flume for which the water tank was partially filled with water and air, enabling free surface movement. Following a 1:40 geometric scale (Armono et al., 2019), the computational domain was set to 5000 mm × 1000 mm × 800 mm (L × W × H). The 500 mm floating prototype, equivalent to 20,000 mm × 6000 mm × 4800 mm in actual scale, was positioned at a water depth of 500 mm, with a 60° mooring angle and a distance of 2675 mm from the inlet.

a. Mesh Generation

Figure 2 shows the three-dimensional model was created in ANSYS DesignModeler and brought in ANSYS Workbench. For meshing, only the surface body was used to allow a two-dimensional analysis, with an automatic meshing method and a manually defined element size of 5 mm.

b. Wave Generation and Boundary Conditions

The wave heights used in this study were those of the Philippine Atmospheric, Geophysical, and Astronomical Services Administration (PAGASA) which were classified into low, moderate, and high wave conditions. Using Froude scaling (1:40), the corresponding model wave heights were 0.0169 m, 0.0656 m, and 0.1625 m for actual wave heights of 0.6750 m, 2.6250 m, and 6.5000 m, with prototype wave periods of 0.47 s, 0.79 s, and 1.26 s, wavelengths of 0.3513 m, 0.9744 m, and 2.4787 m, and frequencies of 2.1082 Hz, 1.2658 Hz, and 0.7937 Hz, respectively.

c. Data Monitoring and Output Parameters

The maximum and minimum values obtained directly from the probe signals were used to determine the incident wave height (Hi) and transmitted wave height (Ht); utilized in the calculation of the wave transmission coefficient (Kt) and wave reduction (%).

Experimental Validation Using Flume Tank Testing

An experiment on a wave flume was carried out in a laboratory-scale to confirm the findings of the numerical simulation by duplicating the same conditions of waves as those that were used in the computational model.

a. Apparatus and Experimental Set-Up

The experimental testing was conducted in a 5000 mm × 1000 mm × 800 mm flume tank equipped with a mechanical paddle wave generator. Water surface elevations were monitored using an Arduino-based data acquisition system and two HC-SR04 ultrasonic sensors positioned above the water surface at a distance of 24 cm.

b. Wave Production and Management.

Wave generation is obtained with the help of mechanical wave maker, and wave properties are adjusted with the help of a programmable wave controller. The simulations are sustained by regular waves via controlled input conditions.

c. Sensor Placement

The wave height was measured by two sensors: Sensor 1 was at 300 mm upstream of the center to measure the initial height (H1), and Sensor 2 was at 300mm downstream to measure the corresponding height (H2), located in accordance with the numerical model and the experimental and simulated results could be compared.

d. Acquisition and averaging of data.

The sensors were attached to an Arduino microcontroller that was programmed to calculate the average of the recorded distances of each sensor during the 30-second period. This was done to the incident and transmitted sensors separately to each trial.

e. Wave Height Determination

Wave heights of the trials were determined by the following equation 3.

$$H_W = 2(H_S - MD_{avg}) \quad \text{- eq. 3}$$

Where:

H_W = Wave height
H_S = Height of the sensor
MD_{avg} = Average measured distance

This procedure was done in each of the three experiments of each case and the mean height of the wave was calculated as:

$$H_{avg} = \frac{\sum_{i=1}^{Nw} Hw}{N_W} \quad \text{- eq 4.}$$

Where:

H_{avg} = Average wave height
H_W = Wave height
N_W = Number of trials

f. Wave Transmission Coefficient

The transmission coefficient of the floating structure was determined as Kt, which is a measure of the proportion of wave energy that passes beyond the floating structure:

$$K_t = \frac{H_t}{H_i} \quad \text{- eq 5}$$

Where:

K_t = Wave transmission coefficient
H_t = Transmitted wave height
H_i = Incident wave height

Kt values below 1 imply that the waves incident are attenuated whereas Kt = 1 approximates that the wave energy is not significantly reduced.

g. Wave Reduction

Wave reduction was expressed as a percentage to evaluate the effectiveness of the structure in dissipating wave energy:

$$WR\ (\%) = \left(1 - \frac{H_t}{H_i}\right) x\ 100 \quad \text{- eq. 6}$$

Where:

WR = Percentage of wave reduction
H_t = Transmitted wave height
H_i = Incident wave height

Positive value implies a good attenuation of the wave, and negative or zero value implies that there is no significant reduction or possibly an increase of the wave heights.

Comparison of Numerical Predictions with Experimental Results Using MAPE

The Mean Absolute Percentage Error (MAPE) was employed to compare the simulated and experimental results and to assess the accuracy of the numerical simulation in predicting the heights of the transmitted waves.

$$MAPE\ (\%) = \frac{1}{n}\sum_{i=1}^{n} \left| \frac{H_{t,num,i} - H_{t,exp,i}}{H_{t,exp,i}} \right| \times 100 \quad \text{- eq. 7}$$

Where:

$H_{t,num,i}$ = Transmitted wave height from numerical simulation for trial
$H_{t,exp,i}$ = Transmitted wave height from experimental measurement for trial
n = number of trials

The interpretation of MAPE values is based on standard practice in wave studies:

- MAPE < 10% - Excellent agreement
- 10% ≤ MAPE ≤ 20% - Good agreement

- 20% < MAPE ≤ 50% - Reasonable agreement
- MAPE > 50% - Poor agreement

This measurement procedure is similar to the methodology used by Ridlwan et al. (2021), who applied the Volume of Fluid (VOF) technique to determine the transmission coefficient of notched-shaped floating breakwaters.

RESULTS

Floating Plastic Composite Mixtures

Design-Expert came up with eleven composite mixtures of different proportions of LDPE, EPS, and treated coconut coir fiber. These mixtures were designated as Mixture Codes 1 to 11.

Finite Element Analysis of Design Mixtures for Compressive Test and Tensile Test Simulation in Fusion 360

The mechanical behavior of different design combinations during uniaxial compressive and tensile loading conditions was evaluated using Fusion 360. Under uniaxial compressive loading (6000 N to 12,000 N), a linear increase in von Mises stress in all design mixtures were observed. Mixture Codes 6 and 9 recorded higher von Mises stress values, ranging from 2.23 MPa to 5.35 MPa, while Mixture Code 11 showed lower stress values. For uniaxial tensile loading (50N to 300N), the maximum von Mises stress values were between 3.11 MPa and 18.59 MPa. Mixtures Code 8 and 9 showed slightly higher stress values than the other mixtures. However, the difference between the tensile responses among all mixtures was minimal.

Fabrication and Experimental Validation of the Floating Plastic Composite Mixtures

a. Fabrication Outcomes

Eleven composite mixtures were fabricated. Of these, seven mixtures (Mixture Codes 1, 2, 3, 4, 6, 8, and 9) were made into solid specimens, and four mixtures (Mixture Codes 5, 7, 10, and 11) failed to be made. Moreover, Control 1 (pure LDPE) and Control 2 (pure EPS) were made successfully.The successfully fabricated mixtures were taken through further physical and mechanical testing.

b. Physical and Mechanical Properties

Table 1 summarizes the physical and mechanical properties of the fabricated composite mixtures.

i. Density

The density of the developed composite mixtures was between 0.6480 g/cm^3 and 0.8480 g/cm^3. The lowest densities were found in Mixture Codes 8 and 9 at 0.6533 g/cm^3 and 0.6480 g/cm^3, respectively. Mixture Code 2 and 4 had the highest densities of 0.8480 g/cm^3 each. Control 1 exhibited a density of 0.7413 g/cm^3, while Control 2 had a density of 0.7680 g/cm^3.

ii. Water Absorption

Water absorption values of the composite mixtures ranged from 0.34% to 7.41%. The lowest values were observed in Mixture Codes 1 and 4, with water absorption of 0.34% and 0.63%, respectively. The highest values were recorded in Mixture Codes 8 and 9, with 7.35% and 7.41%, respectively. Both Control 1 and Control 2 exhibited 0% water absorption.

Table 1. Results of Physical and Mechanical Testing

Mixture Code	Density (g/cm^3)	Water Absorption (%)	Compressive Strength (MPa)	Tensile Strength (MPa)
1	0.7813	0.3400	2.4400	3.1734
2	0.8480	0.9400	2.8400	5.8794
3	0.7040	0.7600	3.0000	8.7425
4	0.8480	0.6300	3.9800	9.5358
6	0.6907	3.0900	4.3500	10.0393
8	0.6533	7.3500	3.8200	18.0890
9	0.6480	7.4100	4.3600	16.5669
C1	0.7413	0.0000	2.9300	8.6700
C2	0.7680	0.0000	4.8600	0.2137

iii. Compressive Strength

The compressive strength of the developed composites ranged from 2.44 MPa to 4.36 MPa. The lowest compressive strength was observed in Mixture Code 1 (2.44 MPa), while the highest values were recorded in Mixture Codes 6 and 9, with 4.35 MPa and 4.36 MPa, respectively. Control 1 and Control 2 had compressive strengths of 2.93 Mpa and 4.86 Mpa, respectively.

iv. Tensile Strength

The tensile strength of the composites that were developed ranged between 3.17 Mpa and 18.09 Mpa. Mixture Code 1 had the lowest value with a tensile strength of 3.17 Mpa. Conversely, Mixture Codes 8 and 9 had the largest tensile strengths of 18.09 MPa and 16.57 MPa respectively. Control 1 had a tensile strength of 8.67 MPa, which is among the control samples. where Control 2 had a significantly smaller value of 0.21 MPa.

c. Validation of Mechanical Simulation Results Using Experimental Compression and Empirical Tensile Data

The compressive and tensile stresses obtained from Autodesk Fusion 360 simulations were compared with experimental results. As shown in Table 2, the compressive tests and maximum von Mises stress ranged from 2.5640–5.1960 MPa, while mean compressive stress ranged from 2.4412–4.8628 MPa. The simulated and experimental values showed good agreement, with absolute errors between 2.64% and 10.29%.

Table 2. Stress Comparison between Uniaxial Simulation and Experimental Compression

Mixture Code	Simulated Load (N)	Average Experimental Load (N)	Maximum Von Misses Stress (MPa)	Average Compressive Stress (Mpa)	Absolute Margin of Error (%)
1	6000	6103	2.5640	2.4412	5.0303
2	7000	7103	3.0440	2.8412	7.1378
3	7000	7500	3.1100	3.0000	3.6667
4	10000	9957	3.5730	3.9828	10.2892
6	10000	10873	4.4640	4.3492	2.6396
8	10000	9550	3.9430	3.8200	3.2199
9	11000	10903	4.6310	4.3612	6.1864
C1	7000	7317	3.0600	2.9268	4.5510
C2	12000	12157	5.1960	4.8628	6.8520

Table 3 shows the tensile test simulation results in comparison to the empirical tensile calculations. The tensile loads applied gave a maximum von Mises stress range of 3.11-18.59 MPa. The average tensile stress ranged from 0.2137 to 18.0890 MPa, while the margin of error ranged from 1.15% to 16.52%

Table 3. Stress Comparison between Uniaxial Simulation and Experimental Tension

Mixture Code	Simulated Load (N)	Average Empirical Load (N)	Maximum Von Misses Stress (MPa)	Average Tensile Stress (MPa)	Absolute Margin of Error (%)
1	50	55.5084	3.1370	3.1734	1.1470
2	100	103.0378	6.2470	5.8794	6.2523
3	150	150.8018	9.3880	8.7453	7.3491
4	150	165.6132	9.3320	9.5358	2.1372
6	150	167.4920	9.3260	10.0393	7.1051
8	300	300.4868	18.5920	18.0890	2.7807
9	250	273.6284	15.4950	16.5669	6.4701
C1	150	152.1133	9.3640	8.6700	8.0046
C2	5	5.1288	0.2560	0.2137	16.5234

Determination and Validation of the Optimal Floating Plastic Composite Mixture

1. Regression Models for Response Prediction

Regression models were created using Response Surface Methodology (RSM), which showed the correlation between components of mixtures and composite responses. The independent variables were LDPE content (A), EPS content (B), and coconut coir fiber content (C). The regression equations of the respective responses are as follows:

Density Model:

$$Density = 0.828463A + 0.750978B - 0.064412C$$

Water Absorption Model:

$$Water\ Absorption = 0.097196A + 0.304332B + 35.60197C$$

Compressive Strength Model:

$$Compressive\ Strength = 3.33071A + 2.47458B + 8.076244C$$

Tensile Strength Model:

$$Tensile\ Strength = 8.69477A + 0.117738B + 56.52301C$$

2. Statistical Modeling and Prediction Using Design-Expert

a. Density

Density results indicate high consistency of experimental and predicted values in all mixtures (0.0306%-11.3350%). Table 4 gives the comparison between experimental and predicted values of the density.

Table 4. Comparison of Experimental and Predicted Density Values

Mixture Code	Actual Value Density	Predicted Value Density	Density RSE
1	0.7813	0.7779	0.4371
2	0.8480	0.8030	5.6040
3	0.7040	0.7940	11.3350
4	0.8480	0.8058	5.2370
6	0.6907	0.7042	1.9171
8	0.6533	0.6535	0.0306
9	0.6480	0.6349	2.0630

b. Water Absorption

Water absorption results showed a great deviation, which is indicative of greater sensitivity to the microstructural variations. Comparison of experimental and predicted water absorption values has been provided in Table 5.

Table 5. Comparison of Experimental and Predicted Water Absorption Values

Mixture Code	Actual Value Water Absorption	Predicted Value Water Absorption	Water Absorption RSE
1	0.3400	0.2324	46.2995
2	0.9400	0.1653	468.6630
3	0.7600	1.0000	24.0000
4	0.6300	0.9691	34.9912
6	3.0900	3.8900	20.5656
8	7.3500	7.0300	4.5519
9	7.4100	7.2400	2.3481

c. Compressive Strength

The results of compressive strength indicate moderate correlation between experimental and predicted compressive strength; the model is performing reasonably within the experimental range. The results of the comparison of the experimental and predicted values of compressive strength are shown in Table 6.

d. Tensile Strength

The tensile strength results are in good agreement with the experimental and the predicted values of tensile strength. Table 7 shows the comparison of experimental and predicted tensile strength values.

Table 6. Comparison of Experimental and Predicted Compressive Strength Values

Mixture Code	Actual Value Compressive Strength	Predicted Value Compressive Strength	Compressive Strength RSE
1	2.4400	2.7700	11.9134
2	2.8400	3.0500	6.8852
3	3.0000	3.3200	9.6386
4	3.9800	3.4600	15.0289
6	4.3500	3.5600	22.1910
8	3.8200	4.3800	12.7854
9	4.3600	4.2500	2.5882

Table 7. Comparison of Experimental and Predicted Tensile Strength Values

Mixture Code	Actual Value Tensile Strength	Predicted Value Tensile Strength	Tensile Strength RSE
1	3.1734	3.0900	2.6990
2	5.8794	5.8700	0.1601
3	8.7425	8.4800	3.0955
4	9.5358	9.7800	2.4669
6	10.0392	10.2600	0.0215
8	18.0890	17.9400	0.8305
9	16.5669	16.600	0.1994

3. Statistical Model Adequacy

The statistical performance of the regression models was evaluated using R^2, adjusted R^2, predicted R^2, F-value, and p-value. Table 8 summarizes the statistical parameters of the developed models.

Table 8. Statistical Summary of Regression Models

	Density	Water Absorption	Compressive Strength	Tensile Strength
R^2	0.7255	0.9742	0.5844	0.9988
Adjusted R^2	0.5883	0.9613	0.3766	0.9982
Predicted R^2	0.3401	0.9399	-0.3892	0.9962
p Value	0.0753	0.0007	0.1727	<0.0001
F Value	5.2900	75.4700	2.8100	1644.48
C.V %	7.5000	21.2800	17.2500	2.23
Standard Deviation	0.0554	0.6239	0.6109	0.2294
PRESS	0.0295	3.6300	4.9900	0.6668

4. Optimization of Mixture Composition

Table 9. Predicted Properties and Desirability of Densified Plastic Composite Mixtures

No.	Density	Water Absorption	Compressive Strength	Tensile Strength	Desirability	
1	**0.8118**	**0.7324**	**3.4190**	**9.4619**	**0.549**	Selected
2	0.8277	0.0993	3.3222	8.609	0.543	
3	0.7897	0.2008	2.9027	4.4063	0.254	

Optimization was performed using Design-Expert software to determine the optimal combination of LDPE, EPS, and coir fiber based on multiple response criteria. Three candidate solutions were created using the software, each having the predicted response values and desirability indices. Out of the solutions generated, the formulation with the highest desirability value (Mixture Code 4) was chosen as the best mixture. The following optimization outcomes are summarized in Table 9.

5. **Validation of Optimal Mixture**

The best combination was also confirmed using experimental testing by comparing the predicted values with the measured ones. Table 10 shows the results of this validation.

Table 10. Validation of the Optimal Mixture

Parameter	Actual Value	Predicted Value	RSE (%)
Density (g/cm³)	0.8480	0.8058	5.2370
Water Absorption (%)	0.6300	0.9691	34.9912
Compressive Strength (MPa)	3.9800	3.4600	15.0289
Tensile Strength (MPa)	9.5358	9.7800	2.4669

Evaluation of Wave Attenuation Performance

The ANSYS Fluent simulations and the experimental results of the flume tank were used to assess the performance of the developed floating composite on the attenuation of the waves. They were measured in terms of incident wave height (Hi), transmitted wave height (Ht), wave transmission coefficient (Kt) and wave reduction (WR).

a. **Numerical Simulation Results**

The results of simulations were invariably reliable in pointing out the decrease in wave height after the encounter with the structure in all the test cases. Table 11 shows incident and transmitted wave heights of all the test cases. The findings indicate that the heights of the transmitted waves (Ht = 18.9000200 mm) were always lower as compared to the incident wave heights (Hi = 20.1000202 mm).

Table 11. Numerical Wave Heights

Test Case	Incident Wave Height (mm)	Transmitted Wave Height (mm)
Case 1 (Low)	20.1000	18.9000
Case 2 (Moderate)	67.1000	62.3000
Case 3 (High)	202.2000	166.3000

The values of the wave transmission coefficient and values of wave reduction are summarized in Table 12. The results show that the value of Kt lies between 0.8225 and 0.9403, and the percentages of the wave reduction are about 5.97 to 17.75.

Table 12. Numerical Wave Transmission Coefficient and Wave Reduction

Test Case	Incident Wave Height (mm)	Transmitted Wave Height (mm)	Wave Transmission Coefficient	Wave Reduction (%)
Case 1 (Low)	20.1000	18.9000	0.9403	5.97
Case 2 (Moderate)	67.1000	62.3000	0.9285	7.15
Case 3 (High)	202.2000	166.3000	0.8225	17.75

b. **Experimental Testing Results**

Table 13. Experimental Wave Heights

Test Case	Incident Wave Height (mm)	Average Incident Wave Height (mm)	Transmitted Wave Height (mm)	Average Transmitted Wave Height (mm)
Case 1 (Low)	20.5060	21.3444	17.0333	18.1857
	21.5712		18.3627	
	21.9559		19.1610	

Test Case	Incident Wave Height (mm)	Average Incident Wave Height (mm)	Transmitted Wave Height (mm)	Average Transmitted Wave Height (mm)
	57.0190		47.2248	
Case 2 (Moderate)	61.9666	59.5974	51.8361	48.3252
	59.8066		45.9148	
	197.9221		137.0041	
Case 3 (High)	173.8639	174.6510	147.4275	128.2463
	152.1668		100.3072	

Table 13 shows the incident and transmitted wave heights recorded. The mean incident wave heights were between 21.3444 mm and 174.6510 mm with the mean transmitted wave height being between 18.1857 mm and 128.2463 mm throughout all the test cases.

Table 14 shows that the wave transmission coefficient (Kt) ranged from 0.7343 to 0.8520, corresponding to wave reduction (WR) values of approximately 14.80% to 26.57%.

Table 14. Experimental Wave Transmission Coefficient

Test Case	Incident Wave Height (mm)	Transmitted Wave Height (mm)	Wave Transmission Coefficient	Wave Reduction (%)
Case 1 (Low)	21.3444	18.1857	0.8520	14.80
Case 2 (Moderate)	59.5974	48.3252	0.8109	18.91
Case 3 (High)	174.6510	128.2463	0.7343	26.57

c. Validation of Numerical Results Using Experimental Data

The level of agreement between the numerical simulations and the experimental measurements of the wave transmission coefficient (Kt) was assessed using the Mean Absolute Percentage Error (MAPE). The absolute percentage error ranged from 10.36% to 14.50% across all cases, while the overall mean absolute percentage error (MAPE) was 12.2902%. Table 15 shows the comparison between numerical and experimental Kt values and the corresponding percentage errors.

Table 15. Comparison of Results and Percentage Error (MAPE)

Test Case	Wave Transmission Coefficient (Simulation)	Wave Transmission Coefficient (Experimental)	Absolute Percentage Error (%)	MAPE (%)
Case 1 (Low)	0.9403	0.8520	10.36	
Case 2 (Moderate)	0.9285	0.8109	14.50	12.2902
Case 3 (High)	0.8225	0.7343	12.00	

DISCUSSION

Fusion 360 showed that the compressive stress of all mixtures were within the reported range (1.35–9.92 MPa) of similar materials reported (Vilane et al., 2021) suggesting consistency with experimentally determined material performance. Similarly, all mixtures were found to have tensile simulation results within the reported tensile strength range (3.024–20.15 MPa) of similar polymer composite materials (Patel & Mehta, 2022; Karaki et al., 2024; Hassan et al., 2025) validating the predicted tensile behavior of the developed mixtures.

The fabrication results show that mixture composition impacts the structural integrity of floating composites. Eleven mixtures yielded seven stable mixtures with adequate LDPE content, while four with less LDPE did not form cohesive structures. This underscores LDPE's importance as the major binding matrix. The developed composites had a density between 0.648 and 0.848 g/cm3. Lower densities occurred in mixtures with more EPS and coconut coir fibre due to air voids and fibre porosity (Mohammed et al., 2025; Sriprom et al., 2022). All mixtures had densities below freshwater (1.00 g/cm3) and seawater (1.02-1.03 g/cm3), ensuring buoyancy.

Compressive and tensile tests simulation were compared to experimental results. The compressive results reveal a linear relationship between applied load and Von Mises Stress, consistent with the polymer composite behavior (Mercado-Colmenero et al., 2023). Errors between simulated and experimental outcomes were attributed to factors such as internal voids, imperfect bonding, and surface friction which could not be represented in the idealized FEA model (Sai et al., 2013). The relative errors for compressive (2.64–10.29%) and tensile (1.15–16.52%) tests were within acceptable ranges reported in previous studies, validating the developed model (Leong et al., 2015; Rahman et al., 2021). The compressive strengths of the composite mixtures lie between 2.44 MPa and 4.36 MPa, tensile strengths lie between 3.17 MPa and 18.09 MPa. The optimization solution found the Mixture Code 4 as an acceptable formulation according to the metric desired (0.5490).

Validation results showed strong agreement between experimental and predicted values for density (RS = 5.2370%), and tensile strength (RSE = 2.4669%) indicating good representation of bulk physical properties and the influence of fiber-reinforcement on tensile performance, while water absorption (RSE = 34.99%) and compressive strength (RSE = 15.03%) exhibited greater variability due to microstructural effects and fiber-alignment (Bam et al., 2023).

The optimized mixture outperformed Control 1, achieving higher tensile strength (9.54 vs. 8.67 MPa) and compressive strength (3.98 vs. 2.93 MPa), with a higher density (0.8480 vs. 0.7413 g/cm³).

Both numerical and experimental results confirmed the wave attenuation capability of the developed floating composite, with wave reduction ranging from 5.97–17.75% for numerical (Kt = 0.8225–0.9403) and 14.80–26.57% for the experimental (Kt = 0.7343–0.8520).

CONCLUSION AND RECOMMENDATIONS

The results indicate that densified LDPE mixed with EPS and coconut coir fiber can be used in floating barrier applications. The resulting mixtures were all characterized by low density, buoyancy, and sufficient strength, which supported their use as floating structures. Both numerical simulations (ANSYS Fluent) and experimental flume tank tests confirmed the prototype's structural integrity and wave attenuation capacity of the prototype developed and the results of both methods were in good agreement.

Further studies are recommended to optimize material composition and structural design to enhance wave attenuation under varying hydraulic conditions and improve moisture resistance and long-term marine durability.

REFERENCES

Anggraini, V., Huat, B. B. K., Asadi, A., & Nahazanan, H. (2014). Effect of coir fibers on the tensile and flexural strength of soft marine clay. *Journal of Natural Fibers*, *12*(2), 185–200. https://doi.org/10.1080/15440478.2014.912973

Armono, H. D., Suastika, K., Ridlwan, A., & Biaperi, T. (2019). Numerical study of bilge keel length variations of floating breakwater to optimize transmission coefficient. In Proceedings of the International Conference on Marine Technology. SciTePress. https://www.scitepress.org/PublishedPapers/2019/100605/100605.pdf

ASTM International. (2019). *ASTM D695-15(2019): Standard test method for compressive properties of rigid plastics.* https://doi.org/10.1520/D0695-15R19

ASTM International. (2020). *ASTM D792-20: Standard test methods for density and specific gravity of plastics by displacement.* https://doi.org/10.1520/D0792-20

ASTM International. (2021). *ASTM D570-98(2021): Standard test method for water absorption of plastics.* https://doi.org/10.1520/D0570-98R21

ASTM International. (2021). *ASTM D790-21: Standard test methods for flexural properties of plastics.* https://doi.org/10.1520/D0790-21

ASTM International. (2022). *ASTM D638-22: Standard test method for tensile properties of plastics.* https://doi.org/10.1520/D0638-22

Bam, S. A., Ajayi, O. O., & Ikpambese, K. K. (2023). Evaluation of Coconut Fibre Reinforced Low Density Polyethylene Composites. *Journal of Engineering Research and Reports*, *24*(12), 45–56. https://doi.org/10.9734/jerr/2023/v24i12859

Climate Tracker Asia. (2024, December 4). *Observed climate trends in the Philippines*. https://climatetracker.asia/observed-climate-trends-in-the-philippines/

Edmonds, D. A., et al. (2020). *Experimental evaluation of floating and submerged coastal protection systems / wave energy dissipation structures*. Ocean Engineering/coastal hydrodynamics literature.

El-meniawy, M. A., Abdelhaleim, A. M., Abdelnaby, A. H., & Saber, D. (2021). Mechanical properties and corrosion behavior of sugarcane bagasse fiber reinforced low density polyethylene composites. Egyptian International Journal of Engineering Sciences and Technology, 36, 63–71. https://eijest.journals.ekb.eg/

Espinach, F. X., Julian, F., Alcalà, M., Vilaseca, F., Carrasco, F., & Mutjé, P. (2023). Effective Tensile Strength Estimation of Natural Fibers through Micromechanical Models: The Case of Henequen Fiber Reinforced-PP Composites. *Polymers*, *14*(22), 4890. ttps://doi.org/10.3390/polhym14224890

Estacio, D. L., et al. (2023). *Wave of change: Revitalization of San Jose Aroma Beach promenade for coastal cultural heritage*. Journal of Research in Technical Design and Development. https://jrtdd.com/index.php/journal/article/view/3688

GMA News Online. (2019, November 11). *Quiel destroys seawall, fishermen's boats in Occidental Mindoro*. https://www.gmanetwork.com/news/topstories/regions/714993/quiel-destroys-seawall-fishermen-s-boats-in-occidental-mindoro/story/

Guruswamy, K. P., Thambiannan, S., Anthonysamy, A., Jalgaonkar, K., Dukare, A. S., Pandiselvam, R., & Jha, N. (2024). Coir fibre-reinforced concrete for enhanced compressive strength and sustainability in construction applications. *Heliyon*, *10*(21), e39773. https://doi.org/10.1016/j.heliyon.2024.e39773

Hassan, F., Eze, W., Umunakwe, R., Oyegoke, T., & Uzochukwu, M. (2025). Physico-mechanical characterization of recycled LDPE blended with EPS as a sustainable rigid alternative to polypropylene. *Cleaner Waste Systems*, *12*, 100383. https://doi.org/10.1016/j.clwas.2025.100383

Hawary, O. E., Boccarusso, L., Ansell, M. P., Durante, M., & Pinto, F. (2023b). An overview of natural fiber composites for marine applications. *Journal of Marine Science and Engineering*, *11*(5), 1076. https://doi.org/10.3390/jmse11051076

Jambeck, J. R., Geyer, R., Wilcox, C., Siegler, T. R., Perryman, M., Andrady, A., Narayan, R., & Law, K. L. (2015). Plastic waste inputs from land into the ocean. *Science*, *347*(6223), 768–771. https://doi.org/10.1126/science.1260352

Karaki, A., Masad, E., Khraisheh, M., & Ouederni, M. (2024). Fused deposition modeling of polyethylene (PE): Printability assessment for low-density polyethylene and polystyrene blends. Composites Part C Open Access, 15, 100499. https://doi.org/10.1016/j.jcomc.2024.100499

Kondo, Y., Arsyad, M., Soenoko, R., & Arman, A. (2023). Effect of alkali solution concentration and soaking time on mechanical properties of coconut fiber. *Archives of* Materials *Science and Engineering*, *124*(2), 1–https://doi.org/10.5604/01.3001.0054.3232

Leong, S., Yusof, Y., & Tan, C. (2015). An experimental and numerical investigation of tensile properties of stone wool fiber reinforced polymer composites. *Advanced Materials Letters*, *6*(10), 888–894. https://doi.org/10.5185/amlett.2015.5835

Mercado-Colmenero, J. M., La Rubia, M. D., Mata-García, E., Rodriguez-Santiago, M., & Martin-Doñate, C. (2023). Using numerical-experimental analysis to evaluate rPET mechanical behavior under compressive stresses and MEX additive manufacturing for new sustainable designs. *Rapid Prototyping Journal*, *29*(11), 98–116. https://doi.org/10.1108/rpj-10-2022-0371

Mohammed, S. A., Alemneh, A. S., Molla, S. W., Krishnan, V., Velmurugan, P., & Adisie, F. B. (2025). Recent progress on the physical, thermal, and mechanical properties of expanded polystyrene waste-based composites. International Journal of Polymer Science. https://doi.org/10.1155/ijps/9285040

NASA Sea Level Change Team. (2024). *Sea level change*. NASA Global Climate Change: Vital Signs of the Planet. https://sealevel.nasa.gov/

Philippine Atmospheric, Geophysical and Astronomical Services Administration (PAGASA). (n.d.). *Weather terminologies*. https://www.pagasa.dost.gov.ph/information/weather-terminologies

Rahman, M. M., et al. (2021). Analytical modeling of composite materials using rule of mixtures and its limitations. *Journal of Materials Engineering and Performance*, 30(5), 3456–3465. https://doi.org/10.1007/s11665-021-05678-4

Reis, M. T., Santos, J. A., & Fazeres-Ferradosa, T. (2025). Advanced studies in breakwaters and coastal protection. *Journal of Marine Science and Engineering*, *13*(2), 370. https://doi.org/10.3390/jmse13020370

Ridlwan, A., Armono, H. D., Rahmawati, S., & Tuswan, T. (2021). Transmission Coefficient Analysis of notched Shape floating breakwater using volume of fluid method: a numerical study. Kapal Jurnal Ilmu Pengetahuan Dan Teknologi Kelautan, 18(1), 41–50. https://doi.org/10.14710/kapal.v18i1.34964

Sai, V. S., Satyanarayana, M. R. S., Murthy, V. B. K., Rao, G. S., & Prasad, A. S. (2013). An experimental simulation to validate FEM to predict Transverse Young's modulus of FRP composites. *Advances in Materials Science and Engineering*, *2013*, 1–6. https://doi.org/10.1155/2013/648527

Sriprom, W., Sirivallop, A., Choodum, A., Limsakul, W., & Wongniramaikul, W. (2022). Plastic/Natural Fiber Composite Based on Recycled EPS Foam Waste. *Polymers, 14*(11), 2241. https://doi.org/10.3390/polym14112241

United Nations Environment Programme. (2022). *From pollution to solution: A global assessment of marine litter and plastic pollution.* https://www.unep.org/resources/report/pollution-solution-global-assessment-marine-litter-and-plastic-pollution

Vilane, B. R. T., Temhlanga, M. S., & Shongwe, M. I. (2021). *The compressive strength of load bearing low density polyethylene (LDPE)-bonded concrete blocks*. Journal of Agricultural Science and Engineering, 7(3), 58–63. http://www.aiscience.org/journal/jase

Vousdoukas, M. I., et al. (2022). Climate change effects on global coastal flood risk. *Nature Communications*, 13, Article 614. https://doi.org/10.1038/s41467-022-28331-2

ACKNOWLEDGMENT

The authors gratefully acknowledge the individuals who contributed significantly to the completion of the study.

DECLARATION OF CONFLICT OF INTEREST

The authors declare no conflict of interest.

DECLARATION OF AI USE

The authors used Grammarly for grammar checking and language editing. All outputs were reviewed and validated by the authors, who take full responsibility for the content.

AUTHOR CRediT STATEMENT

Victoria, L. Y. O.: conceptualization, methodology, software, validation, formal analysis, investigation, data curation, writing-original draft, and writing- review & editing.; **Vargas, E. G.:** conceptualization, methodology, software, validation, formal analysis, investigation, data curation, writing- original draft, and writing- review & editing.; **Malpaya, A. C. V.:** conceptualization, methodology, software, validation, formal analysis, investigation, data curation, writing- original draft, and writing- review & editing.; **Malibiran, G. I.:** conceptualization, methodology, investigation, data curation, writing- original draft, and writing- review & editing.; **Hernandez, N. M.:** conceptualization, methodology, investigation, data curation, writing-original draft, and writing- review & editing.; **Caugma, M. G. L.:** supervision and writing- review & editing.